

Well-developed deformation in  $^{42}\text{Si}$ 

S. Takeuchi,<sup>1,\*</sup> M. Matsushita,<sup>1,2,†</sup> N. Aoi,<sup>1,‡</sup> P. Doornenbal,<sup>1</sup> K. Li,<sup>1,3</sup> T. Motobayashi,<sup>1</sup> H. Scheit,<sup>1,§</sup>  
 D. Steppenbeck,<sup>1,†</sup> H. Wang,<sup>1,3</sup> H. Baba,<sup>1</sup> D. Bazin,<sup>4</sup> L. Càceres,<sup>5</sup> H. Crawford,<sup>6</sup> P. Fallon,<sup>6</sup>  
 R. Gernhäuser,<sup>7</sup> J. Gibelin,<sup>8</sup> S. Go,<sup>9</sup> S. Grévy,<sup>5</sup> C. Hinke,<sup>7</sup> C. R. Hoffman,<sup>10</sup> R. Hughes,<sup>11</sup> E. Ideguchi,<sup>9,‡</sup>  
 D. Jenkins,<sup>12</sup> N. Kobayashi,<sup>13</sup> Y. Kondo,<sup>13</sup> R. Krücken,<sup>7,¶</sup> T. Le Bleis,<sup>14,15,\*\*</sup> J. Lee,<sup>1</sup> G. Lee,<sup>13</sup>  
 A. Matta,<sup>16</sup> S. Michimasa,<sup>9</sup> T. Nakamura,<sup>13</sup> S. Ota,<sup>9</sup> M. Petri,<sup>6,§</sup> T. Sako,<sup>13</sup> H. Sakurai,<sup>1</sup> S. Shimoura,<sup>9</sup>  
 K. Steiger,<sup>7</sup> K. Takahashi,<sup>13</sup> M. Takechi,<sup>1,††</sup> Y. Togano,<sup>1,††</sup> R. Winkler,<sup>4,‡‡</sup> and K. Yoneda<sup>1</sup>

<sup>1</sup>*RIKEN Nishina Center, Wako, Saitama 351-0198, Japan*

<sup>2</sup>*Department of Physics, Rikkyo University, Toshima, Tokyo 172-8501, Japan*

<sup>3</sup>*Peking University, Beijing 100871, People's Republic of China*

<sup>4</sup>*National Superconducting Cyclotron Laboratory, Michigan State University, East Lansing, Michigan 48824, USA*

<sup>5</sup>*Grand Accélérateur National d'Ions Lourds, CEA/DSM-CNRS/IN2P3, F-14076 Caen Cedex 5, France*

<sup>6</sup>*Lawrence Berkeley National Laboratory, Berkeley, California 94720, USA*

<sup>7</sup>*Physik Department, Technische Universität München, D-85748 Garching, Germany*

<sup>8</sup>*LPC-ENSICAEN, IN2P3-CNRS et Université de Caen, F-14050, Caen Cedex, France*

<sup>9</sup>*Center for Nuclear Study, University of Tokyo,*

*RIKEN campus, Wako, Saitama 351-0198, Japan*

<sup>10</sup>*Physics Division, Argonne National Laboratory, Argonne, Illinois 60439, USA*

<sup>11</sup>*Department of Physics, University of Richmond, Richmond, Virginia 23173, USA*

<sup>12</sup>*Physics Department, University of York, Heslington, York YO10 5DD, United Kingdom*

<sup>13</sup>*Department of Physics, Tokyo Institute of Technology, Meguro, Tokyo 152-8551, Japan*

<sup>14</sup>*Institut für Kernphysik, Johann-Wolfgang-Goethe-Universität, D-60486 Frankfurt, Germany*

<sup>15</sup>*GSI Helmholtzzentrum für Schwerionenforschung D-64291 Darmstadt, Germany*

<sup>16</sup>*Institut de Physique Nucléaire, IN2P3-CNRS, Université de Paris Sud, F-91406 Orsay, France*

(Dated: April 15, 2019)

Excited states in  $^{38,40,42}\text{Si}$  nuclei have been studied via in-beam  $\gamma$ -ray spectroscopy with multi-nucleon removal reactions. Intense radioactive beams of  $^{40}\text{S}$  and  $^{44}\text{S}$  provided at the new facility of the RIKEN Radioactive Isotope Beam Factory enabled  $\gamma$ - $\gamma$  coincidence measurements. A prominent  $\gamma$  line observed with an energy of 742(8) keV in  $^{42}\text{Si}$  confirms the  $2^+$  state reported in an earlier study. Among the  $\gamma$  lines observed in coincidence with the  $2^+ \rightarrow 0^+$  transition, the most probable candidate for the transition from the yrast  $4^+$  state was identified, leading to a  $4_1^+$  energy of 2173(14) keV. The energy ratio of 2.93(5) between the  $2_1^+$  and  $4_1^+$  states indicates well-developed deformation in  $^{42}\text{Si}$  at  $N = 28$  and  $Z = 14$ . Also for  $^{38,40}\text{Si}$  energy ratios with values of 2.09(5) and 2.56(5) were obtained. Together with the ratio for  $^{42}\text{Si}$ , the results show a rapid deformation development of Si isotopes from  $N = 24$  to  $N = 28$ .

PACS numbers: 25.60.-t, 23.20.Lv, 27.40.+z, 29.38.Db

Shell closures and collectivity are important properties that characterize the atomic nucleus. Interchange of their dominance along isotopic or isotonic chains has attracted much attention. The recent extension of the research frontier to nuclei far away from the valley of stability has revealed several new phenomena for neutron- or proton-number dependent nuclear structure. For example, a weakening or even disappearance of shell closures occur in several neutron-rich nuclei at  $N = 8$  [1–3] and  $N = 20$  [4–6]. A well known example in the case of  $N = 20$  is the so-called ‘island of inversion’ [7] located around the neutron-rich nucleus  $^{32}\text{Mg}$ . The low excitation energy of the first  $2^+$  state  $E_x(2_1^+)$  and large E2 transition probability [4–6] clearly indicate shell quenching in  $^{32}\text{Mg}$  despite the fact that  $N = 20$  is traditionally a magic number. The next magic number,  $N = 28$ , which appears due to the  $f_{7/2}$ - $f_{5/2}$  spin-orbit splitting, has also been explored [8–13]. Weakening of the shell closure is seen by the decrease of the  $2_1^+$  energy for  $N = 28$  iso-

tones from 3.83 MeV in the doubly-closed nucleus  $^{48}\text{Ca}$  to 1.33 MeV in  $^{44}\text{S}$  as the proton number decreases from  $Z = 20$  to  $Z = 16$ . Another region of shell stability has been shown to exist at  $N, Z = 14$  due to the  $d_{5/2}$ - $d_{3/2}$  spin-orbit splitting. The silicon isotopes from  $^{28}\text{Si}$  to  $^{34}\text{Si}$  exhibit relatively high  $2_1^+$  energies ranging from 1.78 MeV ( $^{28}\text{Si}$ ) to 3.33 MeV ( $^{34}\text{Si}$ ) reflecting the  $Z = 14$  sub-shell closure. However, the  $2_1^+$  energy gradually decreases from  $^{36}\text{Si}$  to  $^{40}\text{Si}$  [12, 14], suggesting a development of quadrupole collectivity for isotopes with  $N > 20$ .

With proton number  $Z = 14$  and neutron number  $N = 28$ , the nuclear structure of  $^{42}\text{Si}$  is of special interest. A simple but important question that arises is whether the weakening of the  $N = 28$  shell closure continues, causing an enhancement of nuclear collectivity, or if shell stability is restored owing to a possible doubly magic structure. A study on  $^{42}\text{Si}$  was made by a two-proton removal reaction experiment with radioactive  $^{44}\text{S}$  beams at the NSCL [15, 16]. The small two-proton

removal cross section was interpreted as evidence for a large  $Z = 14$  sub-shell gap at  $N = 28$ , indicating a nearly spherical shape and a doubly closed-shell structure for  $^{42}\text{Si}$ . Contrary to this result, a disappearance of the  $N = 28$  spherical shell closure around  $^{42}\text{Si}$  was concluded by another experimental study at GANIL with the same reaction [17] owing to the observation of a low-energy  $\gamma$  line interpreted as the transition from the  $2_1^+$  state at 770(19) keV to the ground  $0^+$  state ( $0_{g.s.}^+$ ). This low  $E_x(2_1^+)$  value supports the non-magic nature of  $^{42}\text{Si}$  expected from comparison of the  $\beta$ -decay half-life of  $^{42}\text{Si}$  with QRPA calculations [11].

The disappearance of the  $N = 28$  shell closure for  $^{42}\text{Si}$  was theoretically pointed out in several recent studies with shell-model and mean-field approaches [18–21]. These studies predict a well-developed large deformation of the ground and low-lying states. For further understanding of the structure of  $^{42}\text{Si}$  and, more generally, the mechanism of interchange between the shell closures and quadrupole collectivity along the  $N = 28$  and  $Z = 14$  chains, further experimental input is necessary. In addition to the energy of the  $2_1^+$  state, the location of the  $4_1^+$  state is of crucial importance, since the energy ratio between the  $4_1^+$  and  $2_1^+$  states ( $R_{4/2}$ ) represents the character of quadrupole collectivity: a ratio of 2 is expected for harmonic vibration and 3.33 for rigid-body rotation, as extremes. Hence, the systematic study of  $E_x(2_1^+)$  and  $E_x(4_1^+)$  values is useful to deepen our understanding on the mechanism for the evolution of nuclear structure in the vicinity of  $^{42}\text{Si}$ .

The purpose of the present study is to find the  $4_1^+$  state in  $^{42}\text{Si}$  as well as to revisit the  $2_1^+ \rightarrow 0_{g.s.}^+$  transition. Owing to the secondary  $^{44}\text{S}$  beam with the world-highest intensity provided by the RIKEN Radioactive Isotope Beam Factory (RIBF), population of the  $4_1^+$  state in  $^{42}\text{Si}$  by the two-proton removal reaction was possible, and even a  $\gamma$ - $\gamma$  coincidence analysis was enabled to establish the level scheme with the help of the high-efficiency detector array DALI2 (Detector Array for Low-Intensity radiation 2) [22, 23]. Additionally, we studied multi-nucleon removal reactions of  $^{44}\text{S}$  and  $^{40}\text{S}$  to populate  $4^+$  states in  $^{40}\text{Si}$  and  $^{38}\text{Si}$  in order to obtain valuable information on the evolution of the quadrupole collectivity in neutron-rich Si isotopes provided by the systematic trend of the ratio  $R_{4/2}$ .

The experiment was performed at the RIBF operated by RIKEN Nishina Center and the Center for Nuclear Study, University of Tokyo. Figure 1 shows a schematic view of the setup. A primary  $^{48}\text{Ca}$  beam at 345 MeV/nucleon with an average intensity of 70 pA bombarded a 15-mm-thick rotating beryllium target. A secondary  $^{44}\text{S}$  or  $^{40}\text{S}$  beam was produced by projectile fragmentation and analyzed by the BigRIPS fragment separator [24] as in earlier experiments [25, 26]. The energy and intensity of the secondary  $^{44}\text{S}$  ( $^{40}\text{S}$ ) beam was approximately 210 MeV/nucleon (210 MeV/nucleon) and

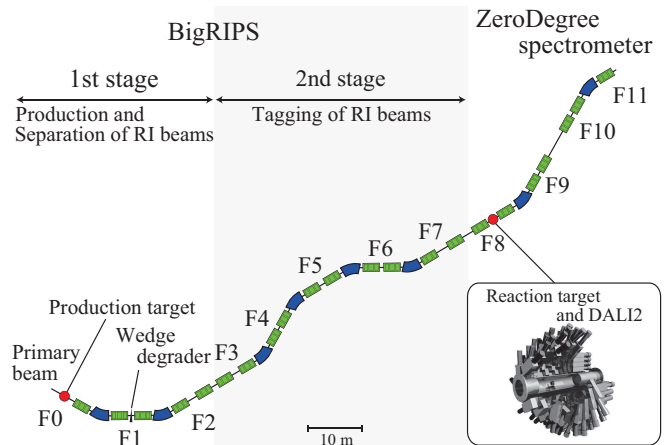


FIG. 1. (Color online) Schematic view of the BigRIPS beam line and the ZeroDegree spectrometer with an illustration of DALI2 located at the F8 focus. The first and second stages of BigRIPS are used for separation and tagging of the secondary beams, respectively.

$4 \times 10^4$  particles per second (pps) ( $6 \times 10^4$  pps), respectively.

A carbon target with a thickness of  $2.54 \text{ g/cm}^2$  was located at the F8 focus (see Fig. 1) for secondary reactions. Reaction products were analyzed using the ZeroDegree spectrometer [27], and identified using the energy loss ( $\Delta E$ ), magnetic rigidity ( $B\rho$ ), and time-of-flight (TOF) information. The  $B\rho$  value was obtained from the position at the dispersive focus F9 measured by parallel plate avalanche counters (PPACs) [28].  $\Delta E$  was measured by an ionization chamber at the achromatic focus F11 and the TOF information was obtained from the time difference between plastic scintillators at F8 and F11.

De-excitation  $\gamma$  rays were detected by the DALI2 array in coincidence with the outgoing  $^{42}\text{Si}$ ,  $^{40}\text{Si}$ , and  $^{38}\text{Si}$  particles. DALI2 consists of 186 NaI(Tl) detectors surrounding the reaction target that cover an angular range of  $11^\circ - 160^\circ$  with respect to the beam axis. Typical photo-peak efficiency and energy resolution are 20% and 10% (FWHM), respectively, for 1 MeV  $\gamma$  rays emitted from nuclei moving with  $\beta (= v/c) \simeq 0.6$ . These values were obtained by Monte-Carlo simulations using the GEANT4 code [29].

Figure 2(a) shows the  $\gamma$ -ray spectrum for the  $\text{C}(^{44}\text{S}, ^{42}\text{Si})\gamma$  reaction, where Doppler-shift effects have been corrected for. For each  $\gamma$ -ray peak, the energy was obtained by a fit of a Gaussian function and an exponential background curve, where the energy resolution was fixed to the simulated value. As seen in the figure, a predominant peak is observed at 742(8) keV, where the error includes statistical and systematic uncertainties. The systematic error is attributed to the uncertainties in the energy calibration (3 keV), the Doppler-shift correction (3 keV), and the ambiguity caused by a delay

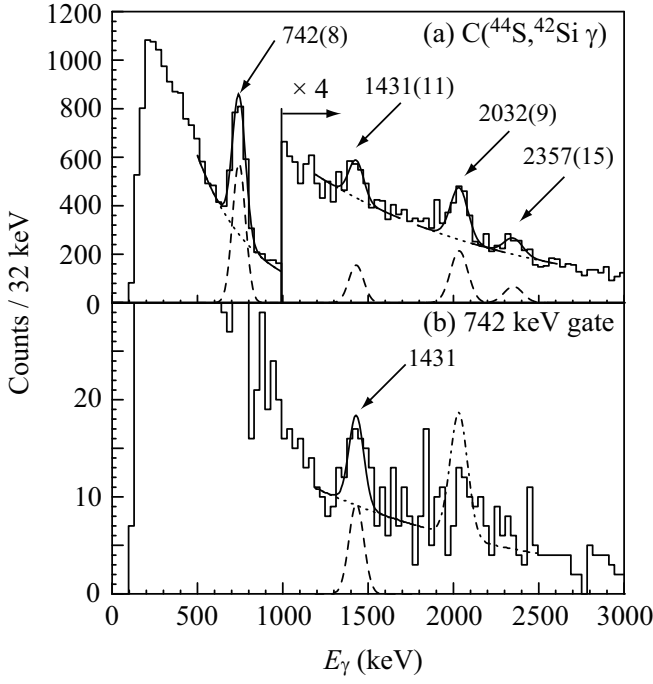


FIG. 2. (a) Doppler-shift corrected  $\gamma$ -ray spectrum obtained for the  $C(^{44}\text{S}, ^{42}\text{Si } \gamma)$  reaction. (b)  $\gamma$ - $\gamma$  coincidence spectrum gated with 742 keV  $\gamma$  ray. Solid curves in both the figures show the results of fits using Gaussian functions (dashed curves) and an exponential curve as the background (dotted curve) by the method  $\chi^2$  minimization. The dot-dashed line indicates the expected line shape in the case that the 2032-keV  $\gamma$  ray decays solely to the  $2_1^+$  state.

of  $\gamma$ -emission resulting in a shift of the source position (estimated to be 2 keV as a maximum lifetime of  $\sim 40$  ps based on systematics [30]). The observed peak energy agrees within 1.5 standard deviation with the value of 770(19) keV reported in the study at GANIL [17]. In the higher energy region, three additional  $\gamma$  lines have been identified in the present study at 1431(11), 2032(9), and 2357(15) keV.

In order to identify the transitions feeding the  $2_1^+$  state, a  $\gamma$ - $\gamma$  coincidence analysis was performed. The spectrum obtained from a gate on the 742-keV line is shown in Fig. 2(b). A clear peak is seen at 1431 keV, which may feed the  $2_1^+$  state directly from a higher-lying excited state at 2173(14) keV. By considering the  $\gamma$ -ray detection efficiency, the yield of the peak is consistent with a 100% feeding of the  $2_1^+$  state. A peak-like structure around  $E_\gamma \simeq 2$  MeV could correspond to the 2032-keV  $\gamma$  line observed in Fig. 2(a), providing another candidate that populates the  $2_1^+$  state. However, the yield of the peak in the  $\gamma$ - $\gamma$  spectrum is lower than the expected value (indicated by the dot-dashed line), based on the intensity measured in Fig. 2(a) and assuming a decay branch of 100% to the level at 742 keV. This suggests that the 2032-keV  $\gamma$  ray does not, or at least does not fully, pop-

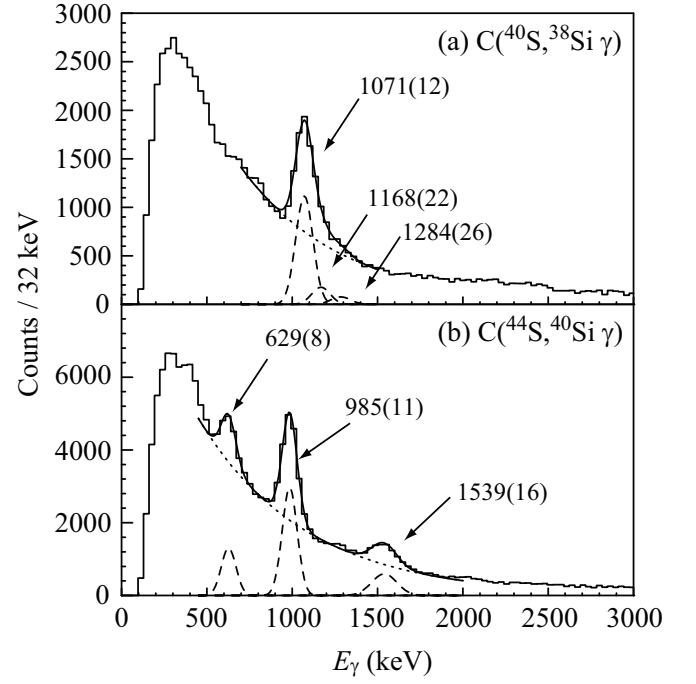


FIG. 3. Doppler-shift corrected  $\gamma$ -ray spectrum obtained in (a) the  $C(^{40}\text{S}, ^{38}\text{Si } \gamma)$  reaction and (b) the  $C(^{44}\text{S}, ^{40}\text{Si } \gamma)$  reaction.

ulate the  $2_1^+$  state. From the known tendency that yrast states, including the  $2_1^+$  and  $4_1^+$  states, are preferentially observed with larger cross sections in nucleon removal reactions [31–33], those two  $\gamma$  lines are possible candidates for the  $4_1^+ \rightarrow 2_1^+$  transition in  $^{42}\text{Si}$ . Since the  $\gamma$ - $\gamma$  coincidence analysis indicates that the 1431-keV  $\gamma$  ray directly feeds the  $2_1^+$  state as discussed above, 2173 (742 + 1431) keV for the  $4_1^+$  energy is more probable among the two possibilities. Thus, we tentatively assign the  $4_1^+$  state at 2173(14) keV. The resultant  $R_{4/2}$  value of 2.93(5) for  $^{42}\text{Si}$  is rather close to the rigid-rotor limit. This contradicts the possibility of a doubly-closed structure suggested by the two magic numbers  $Z = 14$  and  $N = 28$ , but supports enhanced quadrupole collectivity in  $^{42}\text{Si}$  expected from the measured  $2_1^+$  energy [17] and theoretical calculations [18–21]. Furthermore, the large  $R_{4/2}$  value indicates a large static ground state deformation of  $^{42}\text{Si}$ .

A search for  $4_1^+$  states in  $^{38,40}\text{Si}$  was also conducted. Figures 3(a) and (b) show the Doppler-corrected spectra for  $^{38}\text{Si}$  and  $^{40}\text{Si}$ , measured with the  $C(^{40}\text{S}, ^{38}\text{Si } \gamma)$  and  $C(^{44}\text{S}, ^{40}\text{Si } \gamma)$  reactions, respectively. In the case of  $^{38}\text{Si}$ , the major peak likely consists of three unresolved  $\gamma$ -ray lines, according to the ones observed in a previous experiment [13]. Their energies, 1071(12), 1168(22), and 1284(26) keV, were obtained by fitting the spectrum shown in Fig. 3(a), where three peaks with fixed widths and initial centroid positions estimated from Ref. [13] were used in the fitting procedure. The 1071-keV  $\gamma$  line

corresponds to the known  $2_1^+ \rightarrow 0_{g.s.}^+$  transition, while the 1168- and 1284-keV lines are candidates for the  $4_1^+ \rightarrow 2_1^+$   $\gamma$  ray. Here, we assign the 2239-keV state to be the most probable candidate for the  $4_1^+$  state, based on the same arguments of yrast feeding that were discussed for  $^{42}\text{Si}$ . We note that the alternative  $4_1^+$  assignment to the 2355-keV state does not affect the discussion on the systematics of the level energies of Si isotopes discussed later.

For  $^{40}\text{Si}$ , three  $\gamma$  lines are seen at 629(8), 985(11), and 1539(16) keV in Fig. 3(b). The 629- and 985-keV lines have been observed in the  $p(^{42}\text{P}, ^{40}\text{Si} + \gamma)$  reaction. The 985-keV  $\gamma$  ray was assigned to the  $2_1^+ \rightarrow 0_{g.s.}^+$  transition [12]. The line at 1539 keV is reported here for the first time. According to  $\gamma$ - $\gamma$  coincidence analysis, the 629- and 1539-keV  $\gamma$  lines are considered to be transitions from the excited states at 1614(14) and 2524(19) keV to the  $2_1^+$  state. Using similar arguments to those given for  $^{38}\text{Si}$  and  $^{42}\text{Si}$  regarding the preferential population of yrast states, either of the two states could be the yrast  $4^+$  level. However, systematic trends of  $2^+$  and  $4^+$  energies suggest that the level at 2524 keV is the more likely of the two. The 1614-keV state is consistent with the previously observed tentative 1624(7)-keV state [12]. On the basis of the shell model calculations in Ref. [12] this level could be either a  $0^+$  or  $2^+$  level.

Figure 4 shows the isotopic dependence of the excitation energies of the  $2_1^+$  and  $4_1^+$  states together with their ratio  $R_{4/2}$  for  $^{36-42}\text{Si}$ , where filled symbols represent the present results, and open symbols for  $^{36}\text{Si}$  are taken from Ref. [34]. As seen in the figure, the ratios for  $^{36}\text{Si}$  and  $^{38}\text{Si}$  [ $R_{4/2} = 2.024(4)$  and  $2.09(5)$ ] are close to the vibrational limit, suggesting a nearly spherical shape, whereas  $R_{4/2}$  for  $^{40}\text{Si}$  increases to  $2.56(5)$ , indicating a deviation from the spherical shape or enhancement of quadrupole collectivity at  $N = 26$ . The lowering of the  $2_1^+$  energy as well as the increase of the reduced transition probability or the deformation parameter obtained for  $^{36,38,40}\text{Si}$  was interpreted as a narrowing of the  $N = 28$  shell gap [12–14]. The  $0\hbar\omega$  calculation by Nowacki and Poves [20], indicated by the dashed lines in Fig. 4, reproduces  $E_x(2_1^+)$  and  $R_{4/2}$  in a satisfactory manner up to  $^{40}\text{Si}$ , but then deviates significantly from the experimental result for  $^{42}\text{Si}$ . In the case of the  $N = 28$  isotope,  $E_x(2_1^+)$  is lower than  $^{40}\text{Si}$  and  $R_{4/2}$  further increases to  $2.93(5)$  despite the neutron magic number  $N = 28$ . This indicates that a development of nuclear deformation continues up to  $N = 28$ . Also the quadrupole collectivity increase in proton deficient  $N = 28$  isotones turns out to continue to  $^{42}\text{Si}$  with  $Z = 14$ . Thus, for  $^{42}\text{Si}$  well developed deformation has been experimentally established, and the possibility to have a doubly-magic nature was excluded.

The solid lines in Fig. 4 show the results obtained by the Monte-Carlo shell model (MSCM) [18, 19], which includes the tensor force in the effective interaction. The model reproduces the overall trend even for the  $4_1^+$  energies, where better agreement is seen compared with

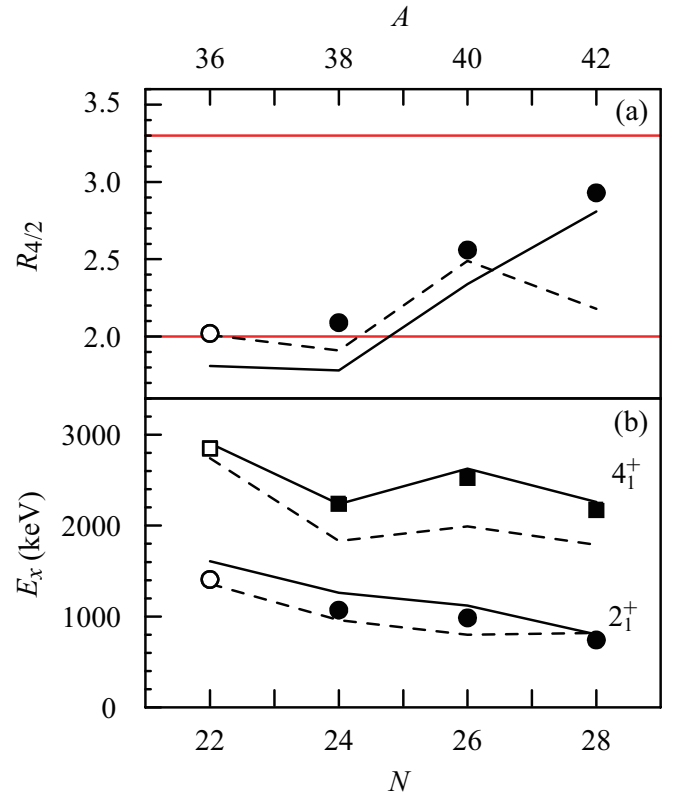


FIG. 4. (Color online) (a) Ratio between the energies of the  $2_1^+$  and  $4_1^+$  states ( $R_{4/2}$ ) for Si isotopes. The red lines at 2.0 and 3.3 indicate the vibrational and rotational limits, respectively. (b) Excitation energies for  $2_1^+$  and  $4_1^+$  states, which are indicated by circles and squares, respectively. Filled symbols are results of the present study, and solid and dashed black lines represent predictions of the MSCM with the tensor force [18, 19] and  $0\hbar\omega$  calculations [20], respectively (see text for details). The  $2^+$  energies of the  $N = 24, 26, 28$  Si isotopes have been measured in previous works [12, 14, 17].

the  $0\hbar\omega$  shell model [20] (dashed lines). In particular, it predicts a large  $R_{4/2}$  value of 2.8 for  $^{42}\text{Si}$ , which is close to  $2.93(5)$  obtained in the present study. The mean field calculation [21] predicts a rotational band in  $^{42}\text{Si}$ . Though the excitation energies of the  $2_1^+$  and  $4_1^+$  states are about two times larger than the experimental values, the  $R_{4/2}$  ratio (2.7) is not far from the present result. It should be noted that the theoretical calculations [19–21] predict an oblate shape of  $^{42}\text{Si}$ . One of the future experiments might be to determine the sign of deformation. Another challenge could be to extend the study to more neutron-rich nuclei, such as  $^{40}\text{Mg}$  and  $^{44}\text{Si}$ , to further trace the quadrupole-collectivity development along the chains of  $N = 28$  isotones and  $Z = 14$  isotopes. Further experimental and theoretical studies are desired for a more profound understanding of the mechanism behind the structure evolution in the vicinity of  $^{42}\text{Si}$ .

In summary, excited states in  $^{38,40,42}\text{Si}$  have been in-

vestigated via in-beam  $\gamma$ -ray spectroscopy with multi-nucleon removal reactions in inverse kinematics by using 210-MeV/nucleon  $^{40,44}\text{S}$  beams. With the high-efficiency detector array DALI2 and the high intensity secondary beams provided at RIKEN RIBF, measurements with high statistics were achieved. The energy of the first  $2^+$  state in  $^{42}\text{Si}$  was measured to be 742(8) keV, and the most probable candidate of the  $4_1^+$  state was found at 2173(14) keV with the aid of a  $\gamma$ - $\gamma$  coincidence analysis. The  $4_1^+$  states in  $^{38}\text{Si}$  and  $^{40}\text{Si}$  were assigned excitation energies of 2239(25) and 2524(19) keV, respectively. The systematics of the ratio  $R_{4/2}$  of the  $4_1^+$  and  $2_1^+$  energies in silicon isotopes from  $N = 24$  to  $N = 28$  shows a rapid development of deformation. The  $R_{4/2}$  value of 2.93(5) for  $^{42}\text{Si}$  is the largest also among the known  $N = 28$  isotones, indicating that this nucleus has a character of well-deformed rotor despite the magic numbers  $N = 28$  and  $Z = 14$ .

We thank the RIBF accelerator staff and BigRIPS team for their operation during the experiment. This work was supported by the DFG (EXC 153, KR 2326/2-1), the U.S Department of Energy under Contact No. DE-AC02-05CH11231 and DE-AC02-06CH11357, and the JUSEIPEN program.

---

\* takesato@riken.jp

† Present address: CNS, University of Tokyo, RIKEN campus, Wako, Saitama 351-0198, Japan

‡ Present address: RCNP, Osaka University, Mihogaoka, Ibaraki, Osaka, 567-0047, Japan

§ Present address: Institut für Kernphysik, Technische Universität Darmstadt, 64289 Darmstadt, Germany

¶ Present address: TRIUMF, 4004 Wesbrook Mall, Vancouver, Canada

\*\* Present address: Physik Department, Technische Universität München, D-85748 Garching, Germany

†† Present address: ExtreMe Matter Institute EMMI and Research Division, GSI Helmholtzzentrum, 64291 Darmstadt, Germany

‡‡ Present address: Los Alamos National Laboratory, Los Alamos, NM 87545, USA

- [1] A. Navin, D. W. Anthony, T. Aumann, T. Baumann, D. Bazin, Y. Blumenfeld, B. A. Brown, T. Glasmacher, P. G. Hansen, R. W. Ibbotson, P. A. Lofy, V. Maddalena, K. Miller, T. Nakamura, B. V. Pritychenko, *et al.*, Phys. Rev. Lett., **85**, 266 (2000).
- [2] H. Iwasaki, T. Motobayashi, H. Akiyoshi, Y. Ando, N. Fukuda, H. Fujiwara, Z. Fulop, K. I. Hahn, Y. Higurashi, M. Hirai, I. Hisanaga, N. Iwasa, T. Kijima, T. Minemura, T. Nakamura, *et al.*, Phys. Lett. B, **481**, 7 (2000).
- [3] H. Iwasaki, T. Motobayashi, H. Akiyoshi, Y. Ando, N. Fukuda, H. Fujiwara, Z. Fulop, K. I. Hahn, Y. Higurashi, M. Hirai, I. Hisanaga, N. Iwasa, T. Kijima, A. Mengoni, T. Minemura, *et al.*, Phys. Lett. B, **491**, 8 (2000).
- [4] C. Detraz, D. Guillemaud, G. Huber, R. Klapisch, M. Langevin, F. Naulin, C. Thibault, L. C. Carraz, and F. Touchard, Phys. Rev. C, **19**, 164 (1979).
- [5] D. Guillemaud-Mueller, C. Detraz, M. Langevin, F. Naulin, M. De Saint-Simon, C. Thibault, F. Touchard, and M. Epherre, Nucl. Phys. A, **426**, 37 (1984).
- [6] T. Motobayashi, Y. Ikeda, Y. Ando, K. Ieki, M. Inoue, N. Iwasa, T. Kikuchi, M. Kurokawa, S. Moriya, S. Ogawa, H. Murakami, S. Shimoura, Y. Yanagisawa, T. Nakamura, Y. Watanabe, *et al.*, Phys. Lett. B, **346**, 9 (1995).
- [7] E. K. Warburton, J. A. Becker, and B. A. Brown, Phys. Rev. C, **41**, 1147 (1990).
- [8] O. Sorlin, D. Guillemaud-Mueller, A. C. Mueller, V. Borrel, S. Dogny, F. Pougheon, K. L. Kratz, H. Gabelmann, B. Pfeiffer, A. Wöhr, W. Ziegert, Y. E. Penionzhkevich, S. M. Lukyanov, V. S. Salamatina, R. Anne, *et al.*, Phys. Rev. C, **47**, 2941 (1993).
- [9] H. Scheit, T. Glasmacher, B. A. Brown, J. A. Brown, P. D. Cottle, P. G. Hansen, R. Harkewicz, M. Hellstrom, R. W. Ibbotson, J. K. Jewell, K. W. Kemper, D. J. Morrissey, M. Steiner, P. Thierolf, and M. Thoennessen, Phys. Rev. Lett., **77**, 3967 (1996).
- [10] T. Glasmacher, B. A. Brown, M. J. Chromik, P. D. Cottle, M. Fauerbach, R. W. Ibbotson, K. W. Kemper, D. J. Morrissey, H. Scheit, D. W. Sklenicka, and M. Steiner, Phys. Lett. B, **395**, 163 (1997).
- [11] S. Grevy, J. C. Angelique, P. Baumann, C. Borcea, A. Buta, G. Canchel, W. N. Catford, S. Courtin, J. M. Daugas, F. de Oliveira, P. Dessagne, Z. Dlouhy, A. Knipper, K. L. Kratz, F. R. Lecolley, *et al.*, Phys. Lett. B, **594**, 252 (2004).
- [12] C. M. Campbell, N. Aoi, D. Bazin, M. D. Bowen, B. A. Brown, J. M. Cook, D. C. Dinca, A. Gade, T. Glasmacher, M. Horoi, S. Kanno, T. Motobayashi, W. F. Mueller, H. Sakurai, K. Starosta, *et al.*, Phys. Rev. Lett., **97**, 112501 (2006).
- [13] C. M. Campbell, N. Aoi, D. Bazin, M. D. Bowen, B. A. Brown, J. M. Cook, D. C. Dinca, A. Gade, T. Glasmacher, M. Horoi, S. Kanno, T. Motobayashi, L. A. Riley, H. Sagawa, H. Sakurai, *et al.*, Phys. Lett. B, **652**, 169 (2007).
- [14] R. W. Ibbotson, T. Glasmacher, B. A. Brown, L. Chen, M. J. Chromik, P. D. Cottle, M. Fauerbach, K. W. Kemper, D. J. Morrissey, H. Scheit, and M. Thoennessen, Phys. Rev. Lett., **80**, 2081 (1998).
- [15] J. Fridmann, I. Wiedenhover, A. Gade, L. T. Baby, D. Bazin, B. A. Brown, C. M. Campbell, J. M. Cook, P. D. Cottle, E. Diffenderfer, D. C. Dinca, T. Glasmacher, P. G. Hansen, K. W. Kemper, J. L. Lecouey, *et al.*, Nature(London), **435**, 922 (2005).
- [16] J. Fridmann, I. Wiedenhover, A. Gade, L. T. Baby, D. Bazin, B. A. Brown, C. M. Campbell, J. M. Cook, P. D. Cottle, E. Diffenderfer, D. C. Dinca, T. Glasmacher, P. G. Hansen, K. W. Kemper, J. L. Lecouey, *et al.*, Phys. Rev. C, **74**, 034313 (2006).
- [17] B. Bastin, S. Grevy, D. Sohler, O. Sorlin, Z. Dombradi, N. L. Achouri, J. C. Angelique, F. Azaiez, D. Baiborodin, R. Borcea, C. Bourgeois, A. Buta, A. Burger, R. Chapman, J. C. Dalouzy, *et al.*, Phys. Rev. Lett., **99**, 022503 (2007).
- [18] T. Otsuka, T. Suzuki, and Y. Utsuno, Nucl. Phys. A, **805**, 127c (2008).
- [19] Y. Utsuno, T. Otsuka, B. A. Brown, M. Honma, T. Mizusaki, and N. Shimizu, (2012), arXiv/1201.4077.
- [20] F. Nowacki and A. Poves, Phys. Rev. C, **79**, 014310

- (2009).
- [21] Z. P. Li, J. M. Yao, D. Vretenar, T. Niksic, H. Chen, and J. Meng, *Phys. Rev. C*, **84**, 054304 (2011).
  - [22] S. Takeuchi, T. Motobayashi, H. Murakami, K. Demichi, and H. Hasegawa, *RIKEN Accel. Prog. Rep.*, **36**, 148 (2003).
  - [23] S. Takeuchi, N. Aoi, T. Motobayashi, S. Ota, E. Takeshita, H. Suzuki, H. Baba, T. Fukui, Y. Hashimoto, K. Ieki, N. Imai, H. Iwasaki, S. Kanno, Y. Kondo, T. Kubo, *et al.*, *Phys. Rev. C*, **79**, 054319 (2009).
  - [24] T. Kubo, *Nucl. Instrum. and Methods Phys. Res., Sect. B*, **204**, 97 (2003).
  - [25] P. Doornenbal, H. Scheit, N. Aoi, S. Takeuchi, K. Li, E. Takeshita, H. Wang, H. Baba, S. Deguchi, N. Fukuda, H. Geissel, R. Gernhauser, J. Gibelin, I. Hachiuma, Y. Hara, *et al.*, *Phys. Rev. Lett.*, **103**, 032501 (2009).
  - [26] N. Kobayashi, T. Nakamura, J. A. Tostevin, Y. Kondo, N. Aoi, H. Baba, S. Deguchi, J. Gibelin, M. Ishihara, Y. Kawada, T. Kubo, T. Motobayashi, T. Ohnishi, N. A. Orr, H. Otsu, *et al.*, (2011), arXiv/1111.7196.
  - [27] Y. Mizoi, T. Kubo, H. Sakurai, K. Kusaka, K. Yoshida, and A. Yoshida, *RIKEN Accel. Prog. Rep.*, **38**, 297 (2005).
  - [28] H. Kumagai, A. Ozawa, N. Fukuda, K. Summerer, and I. Tanihata, *Nucl. Instrum. and Methods Phys. Res., Sect. A*, **470**, 562 (2001).
  - [29] S. Agostinelli, J. Allison, K. Amako, J. Apostolakis, H. Araujo, P. Arce, M. Asai, D. Axen, S. Banerjee, G. Barrand, F. Behner, L. Bellagamba, J. Boudreau, L. Broglia, A. Brunengo, *et al.*, *Nucl. Instrum. and Methods Phys. Res., Sect. A*, **506**, 250 (2003).
  - [30] S. Raman, C. W. Nestor, and P. Tikkanen, *At. Data Nucl. Data Tables*, **78**, 1 (2001).
  - [31] M. Belleguic, M. J. Lopez-Jimenez, M. Stanoiu, F. Azaiez, M. G. Saint-Laurent, O. Sorlin, N. L. Achouri, J. C. Angelique, C. Borcea, C. Bourgeois, J. M. Daugas, C. Donzaud, F. De Oliveira-Santos, Z. Dlouhy, J. Duprat, *et al.*, *Phys. Scr.*, **T88**, 122 (2000).
  - [32] K. Yoneda, H. Sakurai, T. Gomi, T. Motobayashi, N. Aoi, N. Fukuda, U. Futakami, Z. Gacsi, Y. Higurashi, N. Imai, N. Iwasa, H. Iwasaki, T. Kubo, M. Kunibu, M. Kurokawa, *et al.*, *Phys. Lett. B*, **499**, 233 (2001).
  - [33] P. Fallon, E. Rodriguez-Vieitez, A. O. Macchiavelli, A. Gade, J. A. Tostevin, P. Adrich, D. Bazin, M. Bowen, C. M. Campbell, R. M. Clark, J. M. Cook, M. Cromaz, D. C. Dinca, T. Glasmacher, I. Y. Lee, *et al.*, *Phys. Rev. C*, **81**, 041302 (2010).
  - [34] X. Liang, F. Azaiez, R. Chapman, F. Haas, D. Bazzacco, S. Beghini, B. R. Behera, L. Berti, M. Burns, E. Caubrier, L. Corradi, D. Curien, A. Deacon, G. de Angelis, Z. Dombradi, *et al.*, *Phys. Rev. C*, **74**, 014311 (2006).